Original Article

Cardiovascular Remodeling and Metabolic Abnormalities in SHRSP.Z-Lepr^{fa}/IzmDmcr Rats as a New Model of Metabolic Syndrome

Takahiro UENO[1)], Hiroto TAKAGI[1)], Noboru FUKUDA[1),2)], Atsuhiko TAKAHASHI[3)], En-Hui YAO[1)], Masako MITSUMATA[4)], Junko HIRAOKA-YAMAMOTO[5)], Katsumi IKEDA[5)], Koichi MATSUMOTO[1)], and Yukio YAMORI[6)]

The purpose of this study was to evaluate whether the spontaneously hypertensive rat SHRSP.Z-Lepr^{fa}/Izm-Dmcr (SHRSP fatty) is a useful animal model to clarify molecular mechanisms that underlie metabolic syndrome. We investigated histopathologic changes in the cardiovascular organs and metabolic characteristics of SHRSP fatty rats, which are congenic rats from a cross between SHRSP and Zucker fatty (ZF) rats. The aortic wall and cardiac, carotid, and renal arteries from SHRSP and SHRSP fatty rats were thicker than those of ZF rats. The renal cortex in SHRSP and SHRSP fatty rats showed severe glomerulosclerosis. Pancreatic islands in SHRSP fatty and ZF rats showed marked hyperplasia. Steady-state plasma glucose concentrations were higher in SHRSP fatty than in ZF rats. Non-fasting triglyceride levels in SHRSP fatty rats were higher than in ZF rats. DNA synthesis in cultured vascular smooth muscle cells (VSMCs) from SHRSP fatty and SHRSP rats was significantly higher than that in VSMCs from Wistar-Kyoto (WKY) or ZF rats. Levels of platelet-derived growth factor A-chain and transforming growth factor-β1 mRNAs were higher in VSMCs from SHRSP fatty and SHRSP than from ZF rats. Microarray analysis identified five genes that were significantly upregulated and four genes that were significantly downregulated in visceral adipose tissue of SHRSP fatty rats compared with levels in control strains (SHRSP and ZF rats). These findings suggest that the combination of hypertension and obesity accelerates vascular remodeling, dyslipidemia, and insulin resistance in metabolic syndrome. The phenotype of SHRSP fatty is similar to that of human metabolic syndrome, and therefore, studies of these rats may help clarify the molecular mechanisms that underlie metabolic syndrome in humans. (*Hypertens Res* 2008; 31: 1021–1031)

***Key Words*: metabolic syndrome, hypertension, insulin resistance, hyperlipidemia, congenic rat**

Introduction

Metabolic syndrome in association with obesity is a major clinical problem associated with cardiovascular diseases such as atherosclerosis and ischemic heart disease (*1*, *2*). Adipocytes in visceral fat of obese humans secrete a variety of cytokines known as adipocytokines, including tumor necrosis

From the [1)]Division of Nephrology and Endocrinology, Department of Medicine, [3)]Division of Cardiology, Department of Medicine, and [4)]Department of Pathology, Nihon University School of Medicine, Tokyo, Japan; [2)]Advanced Research Institute of Science and Humanities, Nihon University Graduate School, Tokyo, Japan; [5)]Frontier Health Science Forum, Mukogawa Women's University, Nishinomiya, Japan; and [6)]WHO Collaborating Center for Research on Primary Prevention of Cardiovascular Diseases, Kyoto, Japan.

This work was supported in part by a Grant-in-Aid from the Japanese Ministry of Education, Culture, Sports, Science and Technology (N.F.:15590863) and a 2006 Research Grant of the 60th Anniversary Memorial Fund, Nihon University Medical Alumni Association (T.U.).

Address for Reprints: Noboru Fukuda, M.D., Ph.D., Department of Medicine, Nihon University School of Medicine, Oyaguchi-kami 30–1, Itabashi-ku, Tokyo 173–8610, Japan. E-mail: fukudan@med.nihon-u.ac.jp

Received September 14, 2007; Accepted in revised form December 19, 2007.

factor (TNF)-α, plasminogen activator inhibitor (PAI)-1, heparin binding–epidermal growth factor (HB-EGF), angiotensinogen, and leptin (*3*). Adipocytokines are thought to induce insulin resistance and to play roles in the pathogenesis of cardiovascular diseases. Moreover, increases in oxidative stress in metabolic syndrome reportedly cause endothelial damage and atherosclerosis (*4*). To investigate in detail the mechanisms that underlie the pathogenesis of cardiovascular diseases associated with metabolic syndrome, animal models of metabolic syndrome are needed.

Hypertension is a major risk factor for various cardiovascular diseases. Prolonged elevation of high blood pressure damages cardiovascular organs and the renin-angiotensin (RA) system. In particular, the tissue RA system, which is independent of the circulating RA system, causes vascular diseases by inducing oxidative stress, extracellular matrix formation, and expression of growth factors (*5*). Therefore, it is believed that the combination of hypertension and obesity accelerates cardiovascular damage.

Hiraoka-Yamamoto *et al*. (*6*) recently established a new rat model of metabolic syndrome, SHRSP.Z-Lepr^{fa}/IzmDmcr, by crossing stroke-prone, spontaneously hypertensive rat (SHRSP) of the Izumo strain, a genetic model of severe hypertension, with Zucker fatty (ZF) rats. SHRSP fatty rat carry the leptin receptor *OB-Rb* gene mutation found in ZF rats. SHRSP fatty rats become obese and simultaneously develop hypertension. Plasma levels of glucose, insulin, and total cholesterol in SHRSP fatty rats are significantly higher than those in SHRSP and are similar to those in ZF rats. Interestingly, plasma levels of triglycerides and leptin in SHRSP fatty rats are significantly higher than those in SHRSP and ZF rats, suggesting that hypertension enhances the metabolic abnormalities observed in obesity. Thus, the phenotype of SHRSP fatty is similar to that of human metabolic syndrome.

In the current study, to clarify the pathogenesis of metabolic syndrome, we examined histologic changes in cardiovascular organs and metabolic characteristics and visceral adipose tissue gene expression in SHRSP fatty rats.

Methods

Our study conformed to the guidelines published in the "Guide for the Care and Use of Laboratory Animals" of the US National Institutes of Health (NIH Publication No. 85-23, revised 1996). Wistar-Kyoto/Izumo (WKY) and SHRSP/Izumo rats were obtained from the Disease Model Cooperative Research Association (Kyoto, Japan). ZF rats were obtained from Tokyo Experimental Animals (Tokyo, Japan). SHRSP fatty rats were established by crossing SHRSP/Izumo with ZF rats as described previously (*6*). Systolic blood pressure (SBP) was measured by the tail-cuff method. Rats were fasted for 12 h before the beginning of the experiments.

Histologic Examination

Twenty-four week-old WKY, SHRSP, ZF, and SHRSP fatty rats were anesthetized with sodium pentobarbital (Nembutal, 50 mg/kg i.p.; Dainippon Pharmaceutical, Osaka, Japan) and perfused with saline followed by 10% neutral buffered formalin. The brain, aorta, heart, kidney, pancreas, liver, and epididymal fat were removed, and the weight of each organ was determined. Tissue specimens were embedded in paraffin, and 2-μm thick slices were stained with hematoxylin-eosin (HE), Elastica van Gieson, and Masson's Trichrome. Histologic examination was performed by a pathologist without any prior knowledge of the experimental groups. To estimate the total area of the midlayer in about 1 cm of the aorta, small cardiac and small renal arteries, the point counting method with a grid was used in 5 equally spaced sections. To quantify the amount of matrix in glomeruli, 50 glomeruli on each section were selected randomly. The percentage of each glomerulus occupied by mesangial matrix was estimated and assigned a score of 0 to 4 as follows: 0, normal; 1, involvement of up to 25% of the glomerulus; 2, involvement of 25% to 50% of the glomerulus; 3, involvement of 50% to 75% of the glomerulus; or 4, involvement of 75% to 100% of the glomerulus. Grading for the glomerular injury score (GIS) was performed as described previously (*7*). To quantify the tubulointerstitial area, 20 areas in each renal cortex were selected randomly.

Tubulo-interstitial injuries were graded for basement membrane thickening, dilation, atrophy, interstitial inflammation, interstitial fibrosis, tubular necrosis, desquamation, and hydropic degeneration as follows: grade 0, none; grade 1, $<10\%$; grade 2, 10–25% as above; grade 3, 26–50%; grade 4, 51–75%; and grade 5, $>75\%$ in an average of 20 fields per kidney coronal section.

Measurements of Steady-State Plasma Glucose and Steady-State Plasma Insulin Levels

Polyethylene catheters (PE-50, Clay Adams, Parsipanny, USA) were inserted into the femoral vein under light ether anesthesia to obtain blood. Rats were fasted for 12 h before the beginning of the experiments. After bolus injection of 50 mg/kg octreotide (Sandoz, Basel, Switzerland) through the catheter, 16 mg/kg/min of glucose, 5 mU/kg/min of human insulin (Novolin R; Novo Nordisk, Copenhangen, Denmark), and 0.77 mg/kg/min of octreotide were infused through the catheter for 150 min. Blood samples were obtained *via* the femoral catheter to measure plasma glucose and insulin levels. Steady-state plasma glucose (SSPG) and steady-state plasma insulin (SSPI) were the plasma levels of glucose and insulin at 120 min, respectively, and these values were used as an index of insulin resistance.

Table 1. Characteristics of the Four Rat Strains Analyzed

	WKY rats	SHRSP	ZF rats	SHRSP fatty
Body weight (g)	460.0±4.1	348.8±7.5	720.0±8.2$^{\#}$	478.8±41.3$^{\#,*}$
SBP (mmHg)	120.0±5.5	259.3±14.9	153.3±11.9$^{\#}$	202.6±5.8$^{\#,*}$
Organ weight (g/100 g BW)				
Brain	0.50±0.03	0.58±0.02	0.26±0.01	0.39±0.05
Heart	0.35±0.04	0.51±0.03	0.28±0.04$^{\#}$	0.38±0.03$^{\#,*}$
Kidneys	0.39±0.04	0.54±0.04	0.36±0.04	0.45±0.05
Liver	4.12±0.04	4.84±0.52	4.93±1.07	5.81±0.92
Epididymal fat	0.93±0.11	0.60±0.12	1.43±0.12$^{\#}$	0.92±0.07$^{\#,*}$

WKY, Wistar-Kyoto; SHRSP, stroke-prone, spontaneously hypertensive rats; ZF, Zucker fatty; SBP, systolic blood pressure; BW, body weight. $^{\#}p<0.05$ *vs*. SHRSP, $*p<0.05$ *vs*. ZF by Student's *t*-test. All values are the mean±SEM of the four animals.

Cell Culture

Vascular smooth muscle cells (VSMCs) were obtained by explant from aortas of 24-week-old rats of each of the four strains. VSMCs were maintained in Dulbecco's modified Eagle's medium (DMEM) with 10% calf serum (Gibco Life Technologies, Gaithersburg, USA), 100 U/mL penicillin, and 100 mg/mL streptomycin. Experiments were performed on cells between the 5th and 10th passages.

Determination of DNA Synthesis

Quiescent VSMCs were incubated in DMEM containing [^{3}H]thymidine (0.5 mCi/mL) (NEN Research Products, Boston, USA) for 2 h. VSMCs were then washed three times with ice-cold PBS and fixed with 10% trichloroacetic acid, and DNA was extracted with 0.2% SDS/0.2 Eq/L NaOH. [^{3}H]Thymidine incorporation was determined by scintillation spectrophotometry.

RT-PCR Analysis

Total mRNA was extracted from aortic midlayer smooth muscle and cultured VSMCs from 24-week-old rats. Aliquots of mRNA were reverse transcribed into single-stranded cDNA by incubation with avian myeloblastoma virus reverse transcriptase (Takara Biochemicals, Tokyo, Japan).

The primers targeted to *TGF-β1* (*8*), *PDGF A*-chain (*9*), and *bFGF* (*10*) were as previously described. Amplification of 18S ribosomal RNA with sense (5′-CGACGACCCATT CGAACGTCT-3′) and antisense primers (5′-GCTATT GGAGCTGGAATTACCG-3′) served as an internal control. In order to confirm that no genomic DNA was co-amplified by PCR, control RT-PCR experiments without reverse transcriptase were performed using every set of primers, and no product was amplified. PCR was performed using a DNA Thermal Cycler (Perkin-Elmer Cetus, Norwalk, USA). For semiquantative analysis of mRNA, the kinetics of the PCR reaction were monitored; the number of cycles at which the PCR products became detectable on the gel was compared between the different samples (*11*). Serial 10-fold dilutions of cDNA (100, 10 and 1 ng) were amplified; the PCR products became detectable at earlier cycles with increasing amounts of cDNA. PCR was performed for 30 cycles with the following thermal cycle profile: denaturing at 96°C for 45 s, primer annealing at 58°C for 45 s, and primer extension at 72°C for 2 min. PCR products were separated by electrophoresis on 1.5% agarose gels, stained with ethidium bromide, and visualized by ultraviolet illumination.

DNA Microarray Rocedure

Total RNA was obtained from visceral adipose tissue of SHRSP fatty, SHRSP and ZF rats by successive extractions with Trizol and RNeasy Mini Kits (Qiagen, Valencia, USA). The RNA was assessed for quality and quantity with a bioanalyzer (Agilent, Palo Alto, USA). DNA microarray analysis was performed according to the manufacturer's instructions (Affymetrix, Santa Clara, USA). In brief, double-stranded cDNA was synthesized from 10 μg of total RNA by reverse transcription with a SuperScript Choice System (Invitrogen, Carlsbad, USA). Biotinylated cRNA was transcribed from the double-stranded cDNA by T7 RNA polymerase reaction with an RNA Transcript Labeling Kit (Enzo Biochem, Farmingdale, USA), fragmented, and applied to Gene Chips (Rat Genome U34 Neurobiology Array; Affymetrix). After hybridization for 16 h at 45°C, the Gene Chip was washed and labeled with R-phycoerythrin streptavidin by using an Affymetrix Fluidics Station 400. The fluorescent signal intensities were measured with an Affymetrix scanner. Raw data were extracted with Microarray Suite 5 software (Affymetrix) and analyzed with GeneSpring GX software (Agilent). Values below 0.01 were set to 0.01. Each measurement was divided by the 50.0th percentile of all measurements in that sample. Each gene was divided by the median of its measurements in all samples. If the median of the raw values was below 10 then each measurement for that gene was divided by 10 if the numerator was above 10; otherwise the measurement was thrown out.

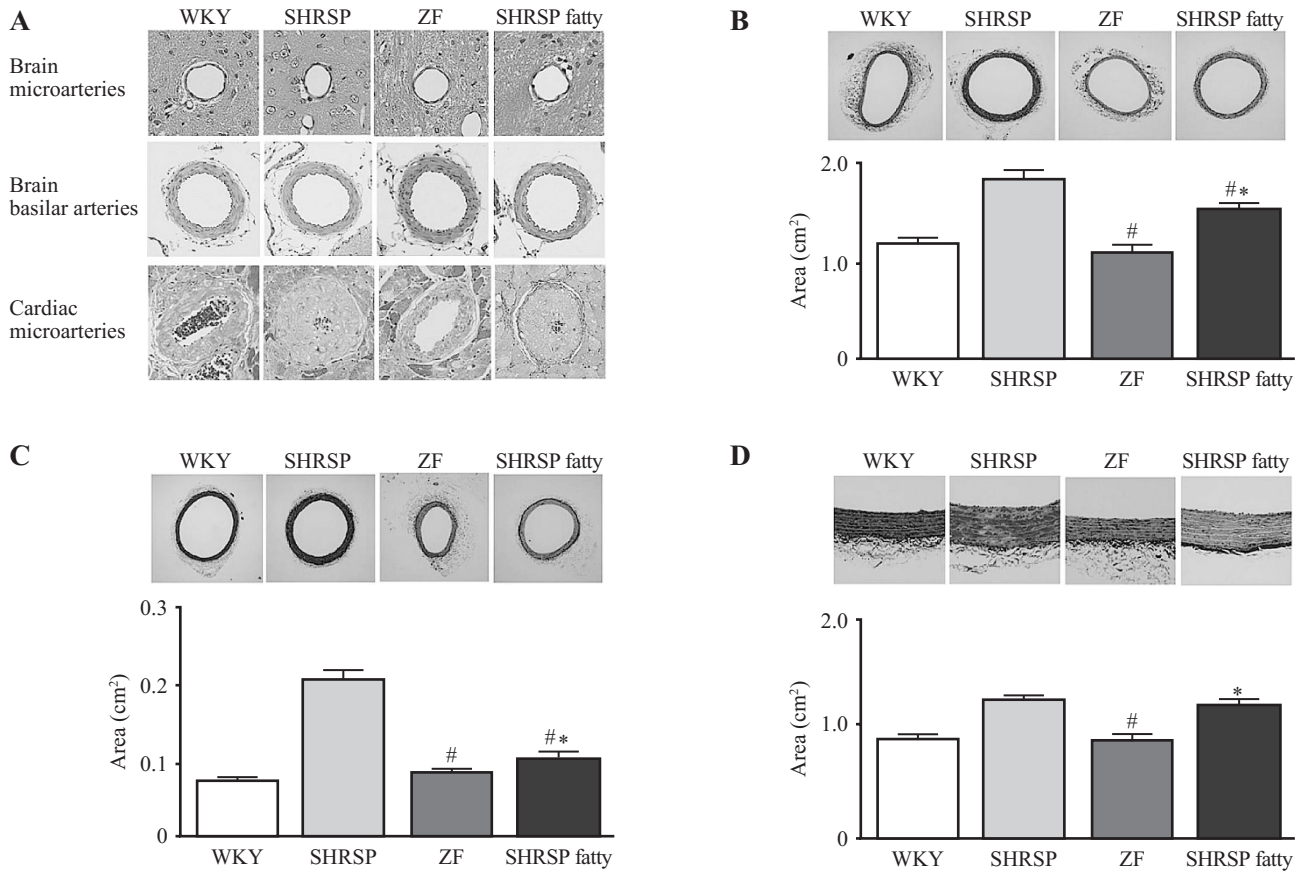

Fig. 1. *Pathologic findings in A: brain microarteries, basilar arteries, cardiac microarteries, B: carotid and C: renal arteries, and D: aortas from 24-week-old Wistar-Kyoto (WKY) rats, stroke-prone, spontaneously hypertensive rats (SHRSP), Zucker fatty (ZF) rats, and SHRSP fatty rats. Sections of brain microarteries and basilar arteries were stained with hematoxylin-eosin. Slices of cardiac microarteries, carotid and renal arteries, and aortas were stained with Masson's Trichrome. Each data point is the mean±SEM of four animals. #$p<0.05$ vs. WKY rats, *$p<0.05$ vs. ZF rats by Student's t-test.*

Statistical Analysis

Results are given as the mean±SEM. The significance of differences between mean values was evaluated by Student's *t*-test for unpaired data. Differences of p less than 0.05 were considered significant.

Results

Characteristics of Four Strains

Body weights, blood pressures, and organ weights of WKY, SHRSP, ZF, and SHRSP fatty rats are shown in Table 1. The mean body weight of SHRSP fatty rats was significantly higher ($p<0.05$) than that of SHRSP and significantly lower ($p<0.05$) than that of ZF rats. SBP in SHRSP fatty rats was significantly lower ($p<0.05$) than that in SHRSP and significantly higher ($p<0.05$) than that in ZF rats. The mean weight of the heart in SHRSP fatty rats was significantly lower ($p<0.05$) than that in SHRSP, whereas it was significantly higher ($p<0.05$) than that in ZF rats. The mean weight of the epididymal fat in SHRSP fatty rats was significantly higher ($p<0.05$) than that in SHRSP and significantly lower ($p<0.05$) than that in ZF rats.

Morphologic Changes in Cardiovascular Organs

Brain microarteries and basilar arteries from 24-week-old WKY, SHRSP, ZF, and SHRSP fatty rats showed similar thicknesses of the midlayer smooth muscle. Cardiac microarteries from SHRSP and SHRSP fatty rats showed vacuolar degeneration in midlayer smooth muscle and multilayered elastic fibers, whereas these changes were not observed in WKY rats or ZF rats (Fig. 1A).

The pathologic changes in large arteries of 24-week-old rats of the four strains are shown in Fig. 1. The thicknesses of the midlayer smooth muscle of the carotid and renal arteries in SHRSP fatty rats were significantly larger ($p<0.05$) than those in ZF rats and lower ($p<0.05$) than those in SHRSP (Fig. 1B and C). The thickness of the midlayer smooth muscle

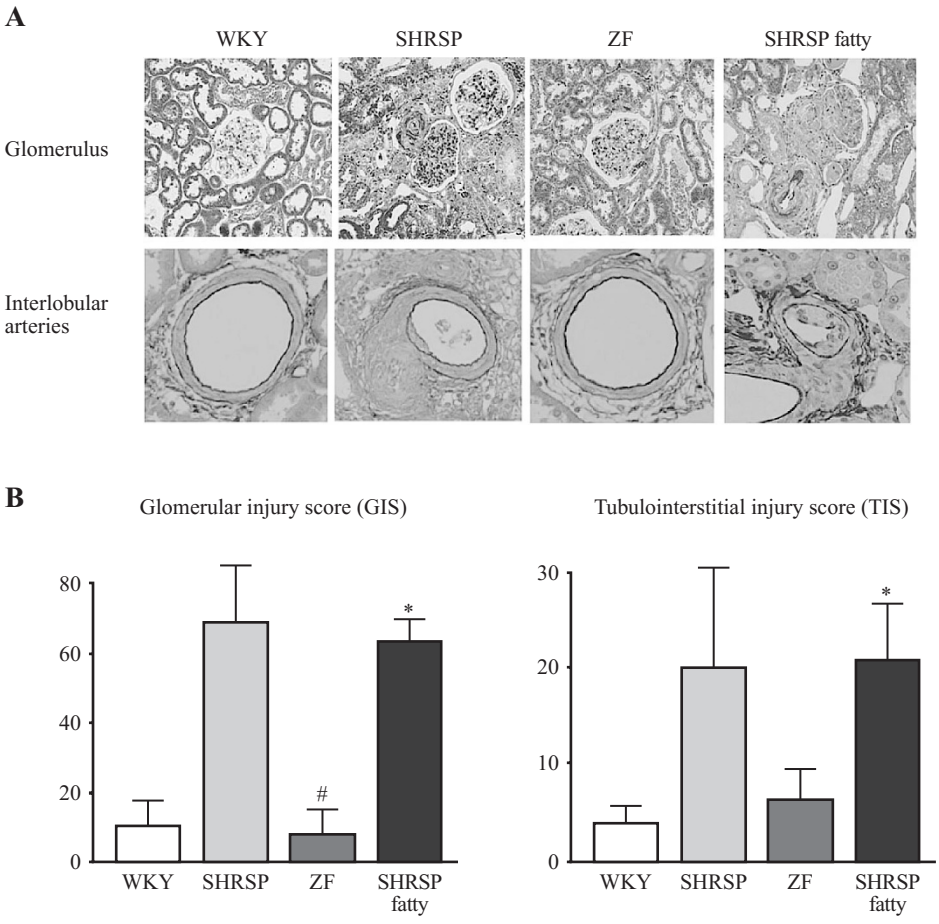

Fig. 2. *Pathologic findings of the renal cortex in 24-week-old Wistar-Kyoto (WKY) rats, stroke-prone, spontaneously hypertensive rats (SHRSP), Zucker fatty (ZF) rats, and SHRSP fatty rats. A: Sections of the glomerulus were stained with hematoxylin-eosin, and sections of interlobular arteries were stained with Elastica van Gieson. B: The glomerular injury score (GIS) and tubulointerstitial injury score (TIS) were determined as described in Methods. Each data point is the mean±SEM of four animals.* $^{\#}p < 0.05$ *vs. WKY rats,* $^{*}p < 0.05$ *vs. ZF rats by Student's t-test.*

of aorta in SHRSP fatty rats was significantly larger than that in ZF rats and similar to that in SHRSP (Fig. 1D).

Pathologic changes in the renal cortex in 24-week-old rats are shown in Fig. 2. Renal cortices from SHRSP and SHRSP fatty rats showed marked thickening of the small artery walls with multiple layers in an "onion skin" pattern, severe glomerulosclerosis with glomerular ischemia due to afferent arterial obstruction, and tubulointerstitial degeneration. Such changes were not observed in WKY and ZF rats (Fig. 2A). GIS and tubulointerstitial injury score (TIS) in SHRSP fatty rats were significantly higher ($p<0.05$) than those in ZF rats and similar to those in SHRSP (Fig. 2B).

Pathologic Findings of the Pancreas and Epididymal Fat in 24-Week-Old Rats

Pancreatic islands in SHRSP fatty and ZF rats showed marked hyperplasia compared to those in the other strains (Fig. 3). The mean sizes of cells in epididymal fat in SHRSP fatty and ZF rats were larger than those of the other strains (Fig. 3).

Metabolic Characteristics

SSPG and SSPI values for the four rat strains are shown in Table 2. SSPG and SSPI values in ZF rats were significantly higher ($p<0.05$) than those in SHRSP. SSPG and SSPI values in SHRSP fatty rats were significantly higher ($p<0.05$) than those in ZF rats.

Plasma lipid profiles of SHRSP, ZF, and SHRSP fatty rats are shown in Table 3. Plasma levels of total cholesterol in ZF rats and SHRSP fatty rats were significantly higher ($p<0.05$) than those in SHRSP. Fasting plasma triglyceride levels were similar among these strains, whereas non-fasting plasma triglyceride levels in ZF rats were significantly higher ($p<0.05$) than those in SHRSP. Non-fasting plasma triglyceride levels

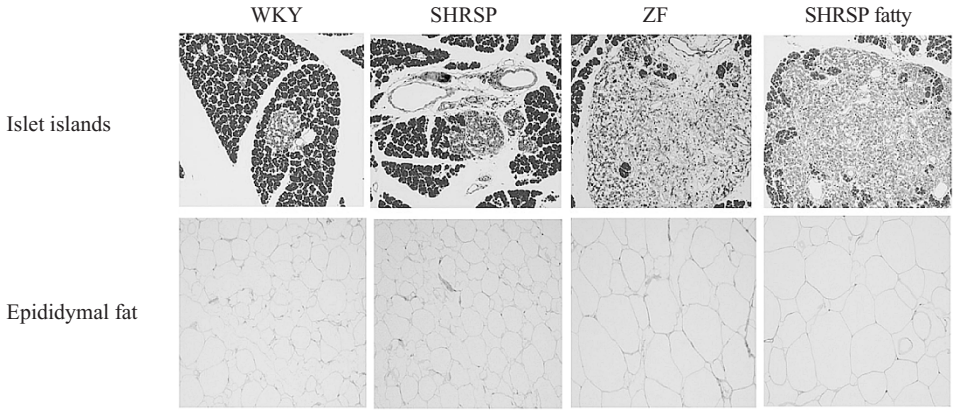

Fig. 3. *Pathologic findings of the pancreas and epididymal fat in 24-week-old Wistar-Kyoto (WKY) rats, stroke-prone, spontaneously hypertensive rats (SHRSP), Zucker fatty (ZF) rats, and SHRSP fatty rats. Each section was stained with hematoxylin-eosin.*

Table 2. Steady-State Plasma Glucose (SSPG) and Steady-State Plasma Insulin (SSPI) Levels of the Four Rat Strains Analyzed

Strain	SSPG (mg/dL)	SSPI (mU/mL)
WKY rats	113.6±11.6	65.8±9.2
SHRSP	109.2±6.5	65.8±18.2
ZF rats	390.9±14.0$^{\#}$	152.7±53.5$^{\#}$
SHRSP fatty	477.9±58.0$^{\#,*}$	308.0±48.5*

SSPG, steady-state plasma glucose; SSPI, steady-state plasma insulin; WKY, Wistar-Kyoto; SHRSP, stroke-prone, spontaneously hypertensive rats; ZF, Zucker fatty. $^{\#}p<0.05$ *vs*. SHRSP, $^{*}p<0.05$ *vs*. ZF by Student's *t*-test. All values are the mean±SEM of the four animals.

in SHRSP fatty rats were significantly higher ($p<0.05$) than those in ZF rats.

Growth Characteristics of VSMCs

To evaluate the growth of VSMCs independently of blood pressure and the metabolic abnormalities of SHRSP fatty rats, we examined basal DNA synthesis and the expression of mRNAs for growth factors in cultured VSMCs derived from the four rat strains. Basal DNA synthesis in VSMCs from SHRSP fatty rats was significantly higher ($p<0.05$) than that in VSMCs from ZF rats and similar to that in VSMCs from SHRSP (Fig. 4A).

Levels of *PDGF A*-chain and *TGF-β1* mRNAs in VSMCs from SHRSP fatty rats were significantly higher ($p<0.05$) than those in VSMCs from ZF rats and similar to those in VSMCs from SHRSP. There was no significant difference in the level of *bFGF* mRNA between VSMCs from the four strains (Fig. 4B).

Gene Expression Profiling of Visceral Adipose Tissue by DNA Microarray

To identify genes differentially expressed between SHRSP fatty rats and the control strains (SHRSP and ZF rats), we carried out microarray analysis. Sixty genes showed significantly higher expression in the visceral adipose tissue of SHRSP fatty rats than in that of SHRSP, including the cannabinoid receptor, 5-hydroxytryptamine receptor, and hypocretin receptor genes. Fifty-three genes showed significantly lower expression in the visceral adipose tissue of SHRSP fatty rats than in that of SHRSP, including the β 3 adrenergic receptor, complement component 3, and thyroid hormone receptor alpha genes. Forty-seven genes were induced at significantly higher levels in the visceral tissue of SHRSP fatty rats compared with that in ZF rats, including the tryptophan hydroxylase, *Fas* and *Metallothionein 1a* genes. The expressions of 48 genes were significantly lower in the visceral tissue of SHRSP fatty rats than in that of ZF rats, including the transforming growth factor β receptor II, interleukin 2 and nitric oxide synthase 2 genes.

Five genes showed remarkable upregulation and four genes showed remarkable downregulation in visceral adipose tissue from SHRSP fatty rats compared with the control strains (SHRSP and ZF rats) (Table 4). The expression of insulin-like growth factor 2 (*IGF2*), like the expressions of metallothionein-2 (*MT-II*), guanine nucleotide binding protein (*GNB1*), cathepsin K (*CTSK*) and heme oxygenase-1 (*HO-1*), was significantly higher in visceral adipose tissue of SHRSP fatty rats than in visceral adipose tissues of the control strains. The expressions of Na^+/K^+ transporting ATPase (*ATP1A2*), superoxide dismutase 3 (*SOD3*), insulin-like growth factor binding protein 2 (*IGF2BP2*) and voltage-dependent anion channel (*VDAC1*) were significantly lower in visceral adipose tissues of SHRSP fatty rats than in those of the control strains. All significant differences in gene expression between SHRSP

Table 3. Plasma Lipid Profiles of SHRSP, ZF Rats, and SHRSP Fatty

Strain		TC (mg/dL)	TG (mg/dL)	HDL (mg/dL)
SHRSP	Non-fasting	61.5±2.5	160.7±8.3	44.2±0.2
	Fasting	50.0±2.3	136.3±15.3	42.5±0.3
ZF rats	Non-fasting	159.3±19.6$^{\#}$	360.5±46.8$^{\#}$	108.4±9.6$^{\#}$
	Fasting	142.5±0.8$^{\#}$	140.3±5.4	86.4±1.5$^{\#}$
SHRSP fatty	Non-fasting	148.5±6.6$^{\#}$	551.5±94.9$^{\#,*}$	40.1±4.9
	Fasting	110.7±23.8$^{\#}$	139.4±15.2	32.0±3.3

TC, total cholesterol; TG, triglyceride; HDL, high-density lipoprotein; SHRSP, stroke-prone, spontaneously hypertensive rats; ZF, Zucker fatty. $^{\#}p<0.05$ *vs*. SHRSP, $^{*}p<0.05$ *vs*. ZF by Student's *t*-test. All values are the mean±SEM of the four animals.

fatty rats and the control strains discovered by microarray analysis were further confirmed by RT-PCR.

Discussion

We investigated histopathologic abnormalities of the cardiovascular organs in 24-week-old SHRSP fatty rats as a new animal model of metabolic syndrome and compared our findings to those in age-matched WKY, SHRSP, and ZF rats. The thickness of the midlayer smooth muscle of the brain microarteries and basilar arteries was similar among the four rat strains. In contrast, the cardiac microarteries from SHRSP and SHRSP fatty rats showed significant thickening of the midlayer smooth muscle with vacuolar degeneration and multilayered elastic fibers. These findings suggest that hypertension and metabolic abnormalities are not associated with hypertrophy of brain arteries, whereas hypertension, but not metabolic abnormalities, induces hypertrophy of cardiac microarteries. Previous studies have shown that salt-loaded SHRSP developed severe hypertension and fibrinoid necrosis of the wall and marked cellular thickening of the intima and media of the arterioles and small arteries of the kidney, testicle, mesentery, adrenal gland, and brain (*12*, *13*). It is possible that the absence of wall thickening in the brain microarteries is due to the fact that we did not salt-load SHRSP fatty and SHRSP rats in the present study.

The thicknesses of the midlayer smooth muscle of the carotid and renal arteries in SHRSP fatty rats were significantly larger than those in ZF rats and smaller than those in SHRSP. These changes were associated with alterations in blood pressure. The thickness of the midlayer smooth muscle of the aorta in SHRSP fatty rats was significantly larger than that in ZF rats and was similar to that in SHRSP. These changes were not correlated with blood pressure, suggesting that these differences may have been related to atherosclerotic changes caused by the metabolic abnormalities.

The renal cortices from SHRSP and SHRSP fatty rats showed marked thickening of the small artery wall with multiple layers in an "onion skin" pattern and severe glomerulosclerosis with glomerular ischemia due to obstruction of the afferent artery. As a result, the GIS levels in SHRSP fatty rats were significantly higher than those in ZF rats and similar to those in SHRSP. These findings suggest that hypertrophy of the small renal arteries and glomerulosclerosis are also associated with hypertension and not with metabolic abnormalities.

ZF rats are resistant to leptin due to a mutation in the leptin receptor, *OB-Rb* (*14*). ZF rats are characterized metabolically by severe insulin resistance with hyperinsulinemia, hyperglycemia, hyperlipidemia, and hypercortisolemia (*15*). In the present study, pancreatic islands in SHRSP fatty and ZF rats showed marked hyperplasia compared to those in WKY rats and SHRSP. The pancreas of ZF rats show pronounced insulin cell hyperplasia, abnormal islet architecture, and lack of pancreatic polypeptide cells (*16*). These changes induce hyperinsulinemia, which reflects insulin resistance (*17*). To examine abnormalities in visceral fat, we measured the size of epididymal fat cells. The mean cell size was larger in SHRSP fatty and ZF rats than in the other strains. Thus, SHRSP fatty rats have abnormalities in the cardiovascular organs, pancreatic islands, and visceral fat that are associated with a combination of hypertension and obesity. To assess insulin resistance, we analyzed SSPG and SSPI in all four strains. SSPG and SSPI values in SHRSP were not different from those in WKY rats. SSPG and SSPI values in ZF rats were significantly higher than those in WKY rats and SHRSP, indicating that ZF rats are resistant to insulin. Interestingly, SSPG and SSPI values in SHRSP fatty rats were higher than those in ZF rats. In addition, non-fasting plasma levels of triglycerides in SHRSP fatty rats were higher than those in ZF rats. These findings suggest that hypertension enhances metabolic abnormalities such as insulin resistance and hypertriglyceridemia in obesity.

The tissue RA system is involved in the pathogenesis of hypertension and insulin resistance (*18–21*). Insulin resistance is observed in non-obese patients with essential hypertension (*1*). Suppression of the RA system with angiotensin converting enzyme (ACE) inhibitors and angiotensin II (Ang II) type 1 receptor antagonists improves insulin resistance in patients with essential hypertension (*22–25*). We previously reported that the tissue RA system is associated with insulin resistance in patients with essential hypertension (*26*). Taken together, these findings indicate that the tissue RA system is associated with hypertension as well as insulin resistance in

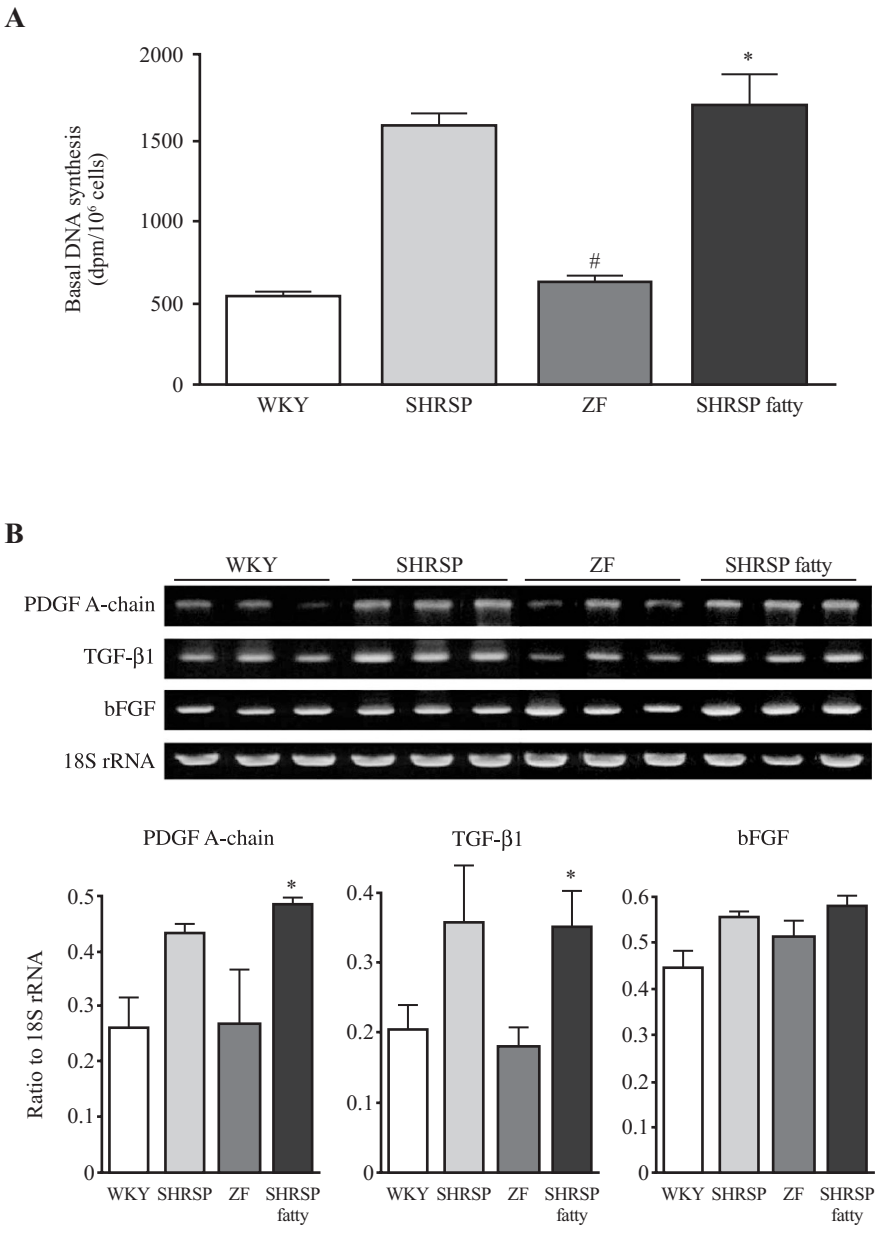

Fig. 4. *Basal DNA synthesis and expression of growth factor mRNAs in cultured vascular smooth muscle cells (VSMCs) derived from Wistar-Kyoto (WKY) rats, stroke-prone, spontaneously hypertensive rats (SHRSP), Zucker fatty (ZF) rats, and SHRSP fatty rats. A: VSMCs became quiescent by incubation in DMEM containing 0.2% calf serum for 48 h, and DNA synthesis was assessed by [^{3}H]thymidine incorporation into DNA. B: Expression of transforming growth factor (TGF)-β1, platelet-derived growth factor (PDGF) A-chain, and basic fibroblast growth factor (bFGF) mRNAs and 18S rRNA was analyzed by reverse transcription–polymerase chain reaction (RT-PCR). The ratio of the abundance of each growth factor mRNA to that of 18S rRNA was calculated. Each data point is the mean ± SEM of four animals. $^{\#}p < 0.05$ vs. WKY rats, $*p < 0.05$ vs. ZF rats.*

patients with essential hypertension. We previously showed that endogenous Ang II suppresses insulin signaling in vascular smooth muscle cells from spontaneously hypertensive rats (SHR) by activating extracellular signal–regulated kinase (*21*). In addition, it has been reported that the tissue RA system induces insulin resistance through oxidative stress induced by activation of NADPH oxidase (*27*, *28*). It has been reported that SHRSP show increased oxidative stress in cardiovascular organs (*29*, *30*). However, in the present study, SHRSP did not show insulin resistance, and this may be due to the fact that these animals have a naturally lower body weight. It is possible that the pathogenesis of hypertension

Table 4. Genes Differentially Expressed in Visceral Adipose Tissue of SHRSP Fatty Rats and Control Rat Strains

Fold change *vs*. ZF	Fold change *vs*. SHRSP	Description
Upregulated genes		
8.048*	2.793#	Insulin-like growth factor 2
3.145*	6.888#	Similar to metallothionein-2
2.913*	2.056#	Guanine nucleotide–binding protein, β 1
2.451*	2.762#	Cathepsin K
2.450*	2.438#	Heme oxygenase 1
Downregulated genes		
0.499*	0.424#	ATPase, Na^+/K^+ transporting, α 2 polypeptide
0.250*	0.216#	Superoxide dismutase 3, extracellular
0.248*	0.402#	Insulin-like growth factor–binding protein 2
0.234*	0.418#	Voltage-dependent anion channel 1

SHRSP, stroke-prone, spontaneously hypertensive rats; ZF, Zucker fatty. #$p<0.05$ *vs*. SHRSP, *$p<0.05$ *vs*. ZF by Student's *t*-test.

increases the activity of the tissue RA system, and the resulting oxidative stress in combination with obesity exacerbates insulin resistance.

Interestingly, SBP in SHRSP fatty rats was lower than that in SHRSP in the present study. It has been reported that the blood pressures of ZF rats is lower than that of lean littermates (*31*, *32*). Thus, the lower blood pressure in SHRSP fatty rats may be associated with leptin resistance.

DNA synthesis in cultured VSMCs from SHRSP fatty and SHRSP rats was significantly higher than that in VSMCs from WKY and ZF rats. The expression of *PDGF A*-chain and *TGF-β1* mRNAs was higher in VSMCs from SHRSP fatty and SHRSP rats than in those from WKY and ZF rats. In culture, cells are not subjected to blood pressure changes. Therefore, the faster growth of VSMCs from SHRSP fatty and SHRSP rats is independent of blood pressure and is therefore related to intrinsic abnormalities. We reported previously that SHR-derived VSMCs in culture show exaggerated growth in comparison to cells from WKY rats, and that SHR-derived VSMCs produce Ang II in homogenous cultures (*33*–*35*). We also reported that the mechanism underlying the enhanced generation of Ang II by VSMCs from SHR appears to be associated with the change from the contractile to the synthetic phenotype, which is accompanied by increases in the numbers of cytosolic organelles (*36*). In addition, we showed that the increased production of Ang II stimulates expression of *PDGF A*-chain and *TGF-β1* (*37*). Therefore, it is possible that the exaggerated growth of VSMCs from SHR, SHRSP, and SHRSP fatty rats and the increased production of growth factors are associated with genetic abnormalities that induce expression of the synthetic phenotype of VSMCs in SHR–related strains.

Adipose tissue is an active endocrine organ that secretes a variety of metabolically important substances, including adipokines. These factors affect insulin sensitivity and may represent a link between obesity and insulin resistance. The DNA microarray approach has been used to identify genes related to the metabolic syndrome phenotype. Sixty genes showed remarkable upregulation and fifty-three genes showed remarkable downregulation in visceral adipose tissue from SHRSP fatty compared with SHRSP rats. However, genes involved in triglyceride metabolism or leptin signaling were not identified as differentially expressed genes between the two strains. We identified five genes, *IGF2*, *MT-II*, *GNB1*, *CTSK*, and *HO-1*, that showed elevated expression in visceral adipose tissue of SHRSP fatty rats compared with that in control strains. We identified four genes, *ATP1A2*, *SOD3*, *IGF2BP2*, and *VDSC1*, that showed reduced expression in visceral adipose tissue of SHRSP fatty rats compared with that in control strains. *IGF2* is a member of the insulin family of polypeptide growth factors, and functions to mediate the activity of growth hormones, stimulate the growth of cultured cells, and stimulate the action of insulin (*38*). The function of *MT-II* is unknown. However, *MT-I* and *-II*–knockout mice are reported to have an obese phenotype (*39*). *IGF2* and *MT-II* may have important roles in the development of visceral obesity. *GNB1* is a heterotrimeric guanine nucleotide–binding protein and transduces extracellular signals received by transmembrane receptors to effector proteins (*40*). Because cells in visceral adipose tissue in obese animals are active, it is reasonable to conjecture that *GNB1* expression is elevated in these cells. Because *HO-1* gene expression is induced by oxidative stress (*41*), upregulation of *HO-1* suggests that oxidative stress may be elevated in the abdominal adipose tissue of SHRSP fatty rats. We also identified four genes that showed lower expression in visceral adipose tissue of SHRSP fatty than in control strains. *ATP1A2* and *SOD3* are known to play important roles in anti-oxidation (*42*, *43*). Reduced expression of these genes may influence atherosclerotic lesion formation in SHRSP fatty rats. *IGF2BP2* binds the leader-3 mRNA in the 5′ untranslated region of *IGF2* and inhibits translation. Downregulation of *IGF2BP2* affects adipose tissue *via* the same axis as observed for upregulation of the *IGF2* gene (*44*). *VDAC1* protein is thought to comprise the major pathway for movement of adenine nucleotides through the outer membrane and to be the mitochondrial binding site

for hexokinase and glycerol kinase (*45*). Glycerol kinase–deficient mice show altered fat metabolism with profound hypertriglyceridemia and elevated free fatty acids (*46*). In our microarray data, most of the genes with altered expression were involved in glucose, lipid, or fat metabolism or oxidative stress. Expression of these genes was altered significantly in SHRSP fatty rats compared with lean SHRSP and fatty ZF rats.

In conclusion, we here demonstrated that SHRSP fatty rats show obesity and hypertension accompanied by hypertrophy of the midlayer smooth muscle of the arterioles, increased non-fasting triglyceride levels, and increased SSPG and SSPI values. These findings suggest that the combination of hypertension and obesity accelerates the vascular remodeling, dyslipidemia, and insulin resistance associated with metabolic syndrome. Therefore, the phenotype of SHRSP fatty rats is similar to that of human metabolic syndrome, and these rats may be a useful tool to investigate the molecular mechanisms that underlie metabolic syndrome. Selected genes with altered expression may play important role in visceral adipose tissue, and further studies are needed to clarify the function of the these genes in metabolic syndrome.

Acknowledgements

We thank Mr. Satoru Tsuchikura of the Disease Model Cooperative Research Association for providing the SHRSP fatty rats.

References

1. Landsberg L: Insulin resistance and hypertension. *Clin Exp Hypertens* 1999; **21**: 885–894.
2. Rett K: The relation between insulin resistance and cardiovascular complications of the insulin resistance syndrome. *Diabetes Obes Metab* 1999; **1** (Suppl 1): S8–S16.
3. Matsuzawa Y, Funahashi T, Nakamura T: Molecular mechanism of metabolic syndrome X: contribution of adipocytokines adipocyte-derived bioactive substances. *Ann N Y Acad Sci* 1999; **892**: 146–154.
4. Eschwege E: The dysmetabolic syndrome, insulin resistance and increased cardiovascular (CV) morbidity and mortality in type 2 diabetes: aetiological factors in the development of CV complications. *Diabetes Metab* 2003; **29**: 6S19–6S27.
5. Schmieder RE, Hilgers KF, Schlaich MP, Schmidt BM: Renin-angiotensin system and cardiovascular risk. *Lancet* 2007; **369**: 1208–1219.
6. Hiraoka-Yamamoto J, Nara Y, Yasui N, Onobayashi Y, Tsuchikura S, Ikeda K: Establishment of a new animal model of metabolic syndrome: SHRSP fatty (fa/fa) rats. *Clin Exp Pharmacol Physiol* 2004; **31**: 107–109.
7. Raij L, Azar S, Keane W: Mesangial immune injury, hypertension, and progressive glomerular damage in Dahl rats. *Kidney Int* 1984; **26**: 137–143.
8. Qian X, Jin L, Grande JP, Lloyd RV: Transforming growth factor-beta and p27 expression in pituitary cells. *Endocrinology* 1996; **137**: 3051–3060.
9. Fukuda N, Kishioka H, Satoh C, *et al*: Role of long-form PDGF A-chain in the growth of vascular smooth muscle cells from spontaneously hypertensive rats. *Am J Hypertens* 1997; **10**: 1117–1124.
10. el-Husseini AE, Paterson JA, Myal Y, Shiu RP: PCR detection of the rat brain basic fibroblast growth factor (bFGF) mRNA containing a unique 3′ untranslated region. *Biochim Biophys Acta* 1992; **1131**: 314–316.
11. Hoof T, Riordan JR, Tummler B: Quantitation of mRNA by the kinetic polymerase chain reaction assay: a tool for monitoring P-glycoprotein gene expression. *Anal Biochem* 1991; **196**: 161–169.
12. Baumbach GL, Walmsley JG, Hart MN: Composition and mechanics of cerebral arterioles in hypertensive rats. *Am J Pathol* 1988; **133**: 464–471.
13. Ogata J, Fujishima M, Tamaki K, Nakatomi Y, Ishitsuka T, Omae T: Stroke-prone spontaneously hypertensive rats as an experimental model of malignant hypertension. I. A light- and electron-microscopic study of the brain. *Acta Neuropathol* (*Berl*) 1980; **51**: 179–184.
14. Takaya K, Ogawa Y, Isse N, *et al*: Molecular cloning of rat leptin receptor isoform complementary DNAs—identification of a missense mutation in Zucker fatty (fa/fa) rats. *Biochem Biophys Res Commun* 1996; **225**: 75–83.
15. Zucker TF, Zucker LM: Fat accretion and growth in the rat. *Obes Res* 1996; **4**: 102–108.
16. Larsson LI, Boder GB, Shaw WN: Changes in the islets of langerhans in the obese Zucker rat. *Lab Invest* 1977; **36**: 593–598.
17. Milburn JL Jr, Hirose H, Lee YH, *et al*: Pancreatic beta-cells in obesity. Evidence for induction of functional, morphologic, and metabolic abnormalities by increased long chain fatty acids. *J Biol Chem* 1995; **270**: 1295–1299.
18. Folli F, Kahn CR, Hansen H, Bouchie JL, Feener EP: Angiotensin II inhibits insulin signaling in aortic smooth muscle cells at multiple levels. A potential role for serine phosphorylation in insulin/angiotensin II crosstalk. *J Clin Invest* 1997; **100**: 2158–2169.
19. Velloso LA, Folli F, Sun XJ, White MF, Saad MJ, Kahn CR: Cross-talk between the insulin and angiotensin signaling systems. *Proc Natl Acad Sci U S A* 1996; **93**: 12490–12495.
20. Fukuda N, Hu WY, Teng J, *et al*: Troglitazone inhibits growth and improves insulin signaling by suppression of angiotensin II action in vascular smooth muscle cells from spontaneously hypertensive rats. *Atherosclerosis* 2002; **163**: 229–239.
21. Fukuda N, Satoh C, Hu WY, Nakayama M, Kishioka H, Kanmatsuse K: Endogenous angiotensin II suppresses insulin signaling in vascular smooth muscle cells from spontaneously hypertensive rats. *J Hypertens* 2001; **19**: 1651–1658.
22. Higashiura K, Ura N, Miyazaki Y, Shimamoto K: Effect of an angiotensin II receptor antagonist, candesartan, on insulin resistance and pressor mechanisms in essential hypertension. *J Hum Hypertens* 1999; **13** (Suppl 1): S71–S74.
23. Shimamoto K, Ura N, Nakagawa M, *et al*: The mechanisms of the improvement of insulin sensitivity by angiotensin converting enzyme inhibitor. *Clin Exp Hypertens* 1996; **18**: 257–266.
24. Bahadir O, Aydin S, Caylan R: The effect on the middle-ear

cavity of an absorbable gelatine sponge alone and with corticosteroids. *Eur Arch Otorhinolaryngol* 2003; **260**: 19–23.
25. Yamaguchi K, Ura N, Murakami H, *et al*: Olmesartan ameliorates insulin sensitivity by modulating tumor necrosis factor-alpha and cyclic AMP in skeletal muscle. *Hypertens Res* 2005; **28**: 773–778.
26. Fukuda N, Nakayama M, Jian T, *et al*: Leukocyte angiotensin II levels inpatients with essential hypertension: relation to insulin resistance. *Am J Hypertens* 2003; **16**: 129–134.
27. Cai H, Li Z, Dikalov S, *et al*: NAD(P)H oxidase–derived hydrogen peroxide mediates endothelial nitric oxide production in response to angiotensin II. *J Biol Chem* 2002; **277**: 48311–48317.
28. Griendling KK, Minieri CA, Ollerenshaw JD, Alexander RW: Angiotensin II stimulates NADH and NADPH oxidase activity in cultured vascular smooth muscle cells. *Circ Res* 1994; **74**: 1141–1148.
29. Moriki N, Ito M, Seko T, *et al*: RhoA activation in vascular smooth muscle cells from stroke-prone spontaneously hypertensive rats. *Hypertens Res* 2004; **27**: 263–270.
30. Negishi H, Ikeda K, Sagara M, Sawamura M, Yamori Y: Increased oxidative DNA damage in stroke-prone spontaneously hypertensive rats. *Clin Exp Pharmacol Physiol* 1999; **26**: 482–484.
31. Mark AL, Shaffer RA, Correia ML, Morgan DA, Sigmund CD, Haynes WG: Contrasting blood pressure effects of obesity in leptin-deficient ob/ob mice and agouti yellow obese mice. *J Hypertens* 1999; **17**: 1949–1953.
32. Verma S, Leung YM, Yao L, Battell M, Dumont AS, McNeill JH: Hyperinsulinemia superimposed on insulin resistance does not elevate blood pressure. *Am J Hypertens* 2001; **14**: 429–432.
33. Fukuda N, Hu WY, Satoh C, *et al*: Contribution of synthetic phenotype on the enhanced angiotensin II–generating system in vascular smooth muscle cells from spontaneously hypertensive rats. *J Hypertens* 1999; **17**: 1099–1107.
34. Fukuda N, Satoh C, Hu WY, *et al*: Production of angiotensin II by homogeneous cultures of vascular smooth muscle cells from spontaneously hypertensive rats. *Arterioscler Thromb Vasc Biol* 1999; **19**: 1210–1217.
35. Hu WY, Fukuda N, Kanmatsuse K: Growth characteristics, angiotensin II generation, and microarray-determined gene expression in vascular smooth muscle cells from young spontaneously hypertensive rats. *J Hypertens* 2002; **20**: 1323–1333.
36. Hu WY, Fukuda N, Satoh C, *et al*: Phenotypic modulation by fibronectin enhances the angiotensin II–generating system in cultured vascular smooth muscle cells. *Arterioscler Thromb Vasc Biol* 2000; **20**: 1500–1505.
37. Satoh C, Fukuda N, Hu WY, Nakayama M, Kishioka H, Kanmatsuse K: Role of endogenous angiotensin II in the increased expression of growth factors in vascular smooth muscle cells from spontaneously hypertensive rats. *J Cardiovasc Pharmacol* 2001; **37**: 108–118.
38. Rodriguez S, Gaunt TR, Day IN: Molecular genetics of human growth hormone, insulin-like growth factors and their pathways in common disease. *Hum Genet* 2007; **122**: 1–21.
39. Beattie JH, Wood AM, Newman AM, *et al*: Obesity and hyperleptinemia in metallothionein (-I and -II) null mice. *Proc Natl Acad Sci U S A* 1998; **95**: 358–363.
40. Hurowitz EH, Melnyk JM, Chen YJ, Kouros-Mehr H, Simon MI, Shizuya H: Genomic characterization of the human heterotrimeric G protein alpha, beta, and gamma subunit genes. *DNA Res* 2000; **7**: 111–120.
41. Calabrese V, Boyd-Kimball D, Scapagnini G, Butterfield DA: Nitric oxide and cellular stress response in brain aging and neurodegenerative disorders: the role of vitagenes. *In Vivo* (*Athens, Greece*) 2004; **18**: 245–267.
42. Katzmarzyk PT, Rankinen T, Perusse L, *et al*: Linkage and association of the sodium potassium-adenosine triphosphatase alpha2 and beta1 genes with respiratory quotient and resting metabolic rate in the Quebec Family Study. *J Clin Endocrinol Metab* 1999; **84**: 2093–2097.
43. Adachi T, Ohta H, Yamada H, Futenma A, Kato K, Hirano K: Quantitative analysis of extracellular-superoxide dismutase in serum and urine by ELISA with monoclonal antibody. *Clin Chim Acta* 1992; **212**: 89–102.
44. Nielsen J, Christiansen J, Lykke-Andersen J, Johnsen AH, Wewer UM, Nielsen FC: A family of insulin-like growth factor II mRNA-binding proteins represses translation in late development. *Mol Cell Biol* 1999; **19**: 1262–1270.
45. Blachly-Dyson E, Zambronicz EB, Yu WH, *et al*: Cloning and functional expression in yeast of two human isoforms of the outer mitochondrial membrane channel, the voltage-dependent anion channel. *J Biol Chem* 1993; **268**: 1835–1841.
46. Huq AH, Lovell RS, Ou CN, Beaudet AL, Craigen WJ: X-linked glycerol kinase deficiency in the mouse leads to growth retardation, altered fat metabolism, autonomous glucocorticoid secretion and neonatal death. *Hum Mol Genet* 1997; **6**: 1803–1809.